0026-895X/04/6604-834–842$20.00
MOLECULAR PHARMACOLOGY
Copyright © 2004 The American Society for Pharmacology and Experimental Therapeutics
Mol Pharmacol 66:834–842, 2004

Vol. 66, No. 4
2956/1174293
Printed in U.S.A.

Molecular Basis for the Differential Agonist Affinities of Group III Metabotropic Glutamate Receptors

Erica Rosemond, Minghua Wang, Yi Yao, Laura Storjohann, Thomas Stormann, Edwin C. Johnson, and David R. Hampson

Department of Pharmaceutical Sciences and Institute for Drug Research, University of Toronto, Toronto, Ontario, Canada (E.R., M.W., Y.Y., D.R.H.); NPS Pharmaceuticals, Salt Lake City, Utah (L.S., T.S.); and AstraZeneca Pharmaceuticals, Wilmington, Delaware (E.C.J.)

Received May 18, 2004; accepted July 1, 2004

ABSTRACT

Agonist stimulation of group III metabotropic glutamate receptors (mGluRs) induces an inhibition of neurotransmitter release from neurons. The group III mGluRs are pharmacologically defined by activation with the glutamate analog L-amino-4-phosphonobutyric acid (L-AP4). The affinities of these receptors for L-AP4 and glutamate vary over approximately a 1500-fold concentration range. The goal of this study was to elucidate the molecular basis for this dispersion of agonist affinities for the group III receptors mGluR4, mGluR6, and mGluR7. [^{3}H]L-AP4 binding was present in human embryonic kidney cells transfected with the high-affinity mGluR4 receptor but not in cells transfected with mGluR6 or the low-affinity mGluR7 receptor. Analysis of mGluR4/mGluR6 receptor chimeras revealed that replacement of the first 35 amino acids of mGluR6 with the first 50 amino acids of mGluR4 was sufficient to impart [^{3}H]L-AP4 binding to mGluR6. Homology models of mGluR4 and mGluR7 were used to predict amino acids that may affect ligand affinity. Mutations were made in mGluR7 to convert selected residues into the equivalent amino acids present in the high-affinity mGluR4 receptor. The mGluR7 N74K mutation caused a 12-fold increase in affinity in a functional assay, whereas the N74K mutation in combination with mutations in residues 258 to 262, which lie outside the binding pocket, caused a 112-fold increase in affinity compared with unmutated mGluR7. Our results demonstrate that the binding site residues at position lysine 74 in mGluR4, glutamine 58 in mGluR6, and asparagine 74 in mGluR7 are key determinants of agonist affinity and that additional residues situated outside of the binding pocket, including those present in the extreme amino terminus, also contribute to agonist affinity and the pharmacological profiles of the group III mGluRs.

The group III metabotropic glutamate receptors (mGluRs; mGluR4, -6, -7, and -8) share 70 to 74% amino acid identity and are selectively activated by the synthetic agonist L-amino-4-phosphonobutyric acid (L-AP4) and the endogenous amino acid L-serine-O-phosphate (L-SOP) (Fig. 1). The mGluR4, mGluR7, and mGluR8 receptor subtypes are expressed primarily on nerve terminals where they act to inhibit neurotransmitter release in the central and peripheral nervous systems (Macek et al., 1996; Pekhletski et al., 1996; Shigemoto et al., 1996; Lafon-Cazal et al., 1999). mGluR6 expression is restricted to retinal bipolar cells, in which it acts postsynaptically to regulate visual responses (Nomura et al., 1994). Animal models have suggested mGluR4 as a potential drug target for the treatment of absence epilepsy (Snead et al., 2000), neurodegenerative disorders associated with overactivation of glutamate-gated ion channels (Bruno et al., 2000), and Parkinson's disease (Marino et al., 2003), whereas mGluR7 may be a potential target for the development of novel antidepressants (Cryan et al., 2003).

Agonists at mGluRs bind to a site localized within the Venus flytrap domain of the extracellular region and induce a conformational change that results in the closure of the flytrap and propagation of the signal through the transmembrane domain (Bessis et al., 2002; Jingami et al., 2003). Although the group III receptors have high-sequence homology, their affinities for L-AP4, L-SOP, and L-glutamate span a wide concentration range encompassing several orders of magnitude. This large dispersion of affinities for endogenous ligands suggests that the group III receptors have evolved to operate over a wide range of intensities of synaptic activity.

Biochemical assays measuring receptor activation together

This work was supported by an operating grant (to D.R.H.) and a PDF Strategic Training grant (to M.W.) from the Canadian Institutes of Health Research, and an Ontario Graduate Scholarship (to E.R.).

Article, publication date, and citation information can be found at http://molpharm.aspetjournals.org.

doi:10.1124/mol.104.002956.

ABBREVIATIONS: mGluR, metabotropic glutamate receptor; CaSR, calcium-sensing receptor; HEK, human embryonic kidney; L-AP4, L-amino-4-phosphonobutyric acid; L-SOP, L-serine-*O*-phosphate; MG-132, *N*-benzoyloxycarbonyl (*Z*)-Leu-Leu-leucinal.

with radioligand binding assays using [^{3}H]L-AP4 have shown that mGluR4 and mGluR8 have similar high affinity for L-AP4 (EC_{50} = 0.4–1 μM, IC_{50} = 0.4–0.8 μM) (Hampson et al., 1999; Han and Hampson, 1999; Schoepp et al., 1999; Peltekova et al., 2000). As expected from the reported low affinity of L-AP4 for mGluR7 in functional assays (EC_{50} = 160–800 μM) (Okamoto et al., 1994; Saugstad et al., 1994; Corti et al., 1998), no specific binding of [^{3}H]L-AP4 was detected in cells expressing mGluR7 (Naples and Hampson, 2001). It is surprising however that despite reports indicating that mGluR6 has a pharmacological profile similar to mGluR4 and mGluR8 in functional assays (i.e., high affinity for L-AP4, EC_{50} = 0.6–0.9 μM) (Nakajima et al., 1993; Ahmadian et al., 1997), no specific binding of [^{3}H]L-AP4 was detected human embryonic kidney (HEK) 293 cells transfected with either rat or human mGluR6 (Naples and Hampson, 2001).

Previous studies have determined that the selectivity of L-AP4 and L-SOP for mGluR4 is conferred by several positively charged amino acids within the ligand binding pocket that interact with the negatively charged phosphonate moiety of these compounds (Bertrand et al., 2002; Rosemond et al., 2002; Macchiarulo et al., 2003). In the present study, the molecular basis for the differential affinities and agonist binding properties of mGluR4, mGluR6, and mGluR7 was investigated. Our results demonstrate that a specific subset of residues located within and just outside of the binding pocket is responsible for the wide range of agonist affinities, and that the extreme amino terminal amino acid sequence is critical for imparting high-affinity [^{3}H]L-AP4 binding.

Materials and Methods

Materials. L-AP4, [^{3}H]L-AP4 (specific activity, 49 Ci/mmol), and L-SOP were purchased from Tocris Cookson Inc. (Ellisville, MO). The anti-mGluR4a and anti-mGluR7a antibodies were purchased from Upstate USA, Inc. (Charlotesville, VA). The anti-mGluR6 antibody was purchased from Neuromics Inc. (Northfield, MN).

Expression Constructs and Site-Directed Mutagenesis. The wild-type rat mGluR4a was subcloned into pcDNA3.1/myc-His (Invitrogen, Carlsbad, CA) as described previously (Rosemond et al., 2002). The mGluR4a with a c-myc epitope inserted between amino acids lysine 35 and glycine 36 was subcloned into pcDNA3 (Invitrogen), as described previously by Han and Hampson (1999). The rat mGluR6 was subcloned into the HindIII and NotI sites of the pcDNA3 vector and the pcDNA3.1 vector. The wild-type rat mGluR7 was subcloned into pcDNA3.1/myc-His vector. The human calcium-sensing receptor (CaSR)-mGluR7 cDNA construct was generated by replacing the first 44 amino acids of the human mGluR7 with the first 27 amino acids of the human CaSR; the cDNA was subcloned into the NheI and NotI sites of the pIREShyg3 vector (BD Biosciences Clontech, Palo Alto, CA).

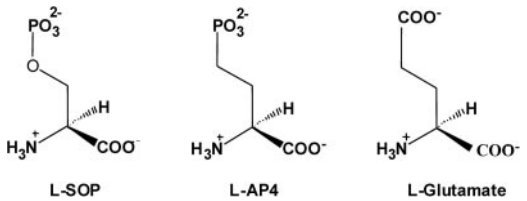

Fig. 1. Structures of the group III mGluR agonists. The synthetic compound L-AP4 has higher affinity for group III mGluRs compared with the endogenous amino acids L-glutamate and L-SOP. The phosphonate functional group on L-AP4 and L-SOP confers selectivity for the group III mGluRs.

A series of chimeras between mGluR4 and mGluR6 were produced in the mGluR6-c-myc background (in pcDNA3.1/myc-His). Restriction enzyme sites at equivalent positions in the cDNAs of mGluR4 and mGluR6 were used to construct the chimeric receptors. The restriction enzyme sites either pre-existed within the cDNAs or were introduced through site-directed mutagenesis. Base-pair changes were produced using the QuikChange site-directed mutagenesis strategy (Stratagene, La Jolla, CA). The 4/6A chimera ($mGluR4_{1–586}$/$mGluR6_{579–871}$) used the SrfI site to exchange the entire amino termini of the two receptors. The introduction of the SrfI site resulted in two amino acid changes in each receptor (P586A and W587R in mGluR4 and P579A and W580R in mGluR6). The 4/6B chimera ($mGluR4_{1–110}$/$mGluR6_{95–871}$) used the XhoI restriction enzyme site, and the 4/6C chimera ($mGluR4_{1–78}$/$mGluR6_{63–871}$) used an alternate XhoI restriction enzyme site. The pre-existing XhoI site within mGluR4 was deleted to produce the 4/6C chimera, whereas the 4/6D chimera ($mGluR4_{1–50}$/$mGluR6_{35–871}$) used the AvrII restriction enzyme site. A second series of chimeras between mGluR4 and mGluR7 were produced within the mGluR7-c-myc background (pcDNA3.1/myc-His). Restriction enzyme sites at equivalent positions in the cDNAs of mGluR4 and mGluR7 were used to construct the chimeric receptors. The 4/7A chimera ($mGluR4_{1–315}$/$mGluR7_{317–915}$) used the BamHI site, the 4/7B chimera ($mGluR4_{1–286}$/$mGluR7_{288–915}$) used the NruI site, the 4/7C chimera ($mGluR4_{1–221}$/$mGluR7_{222–915}$) used the SalI site, and the 4/7D chimera ($mGluR4_{1–110}$/$mGluR7_{109–915}$) used the XhoI restriction enzyme site. All of the single- and multiple-point mutations in mGluR7 were made on the modified CaSR-mGluR7 construct described above. All chimeras and mutants were sequenced before analysis.

Cell Culture and Transfections. HEK293-TSA201 cells were cultured in minimal essential medium supplemented with 6% fetal bovine serum, 2 mM glutamine, and penicillin-streptomycin antibiotics (Invitrogen). For radioligand binding assays, transient transfections of HEK cells were conducted using a calcium phosphate precipitation protocol as described previously (Han and Hampson, 1999). For functional assays, transient transfections of HEK cells were conducted using the LipofectAMINE 2000 reagent (Invitrogen) in 6-well microtiter plates. Receptor cDNA (2 μg) was cotransfected with 1 μg of the cDNA coding for Gα15 per well.

Radioligand Binding. Membranes were harvested 48 h after transfection and were prepared as described previously (Naples and Hampson, 2001; Rosemond et al., 2002). Frozen membranes were thawed and homogenized using a Polytron. Membrane protein (125 μg) was used for all binding assays in a final volume of 250 μl. All assays were performed on ice using 30 nM [^{3}H]L-AP4. Nonspecific binding of this ligand to cell membranes was defined as binding in the presence of 300 μM L-SOP. After a 30-min incubation, bound and free radioligands were separated by centrifugation (14,000*g* for 4 min). The membranes were washed with cold (4°C) assay buffer, solubilized overnight in 1M NaOH, and dissolved in Ultima Gold liquid scintillation fluid before counting on a Tri-Carb 2100TR liquid scintillation analyzer (both from PerkinElmer Life and Analytical Sciences, Boston, MA).

Functional Assay for mGluRs. Responses to L-AP4 were measured in HEK cells loaded with the calcium-sensitive dye Fluo-4 in a fluorescence-based assay as described previously (Kuang et al., 2003; Yao et al., 2003). The fluorescence-induced calcium release was recorded on a FLEXstation benchtop scanning fluorometer (Molecular Devices, Sunnyvale, CA) at room temperature with settings of 485 nm for excitation and 525 nm for emission. For mGuR7, we found that at L-AP4 concentrations of ≥1 mM, responses were seen in mock-transfected HEK cells. Therefore in the calculation of the EC_{50} value for mGluR7, the responses observed at high L-AP4 concentrations in mock transfected cells were subtracted from the responses obtained in mGluR7-transfected cells. The GraphPad Prism 3.0 software was used to plot fluorescence intensities and calculate EC_{50} values (GraphPad Software Inc., San Diego, CA).

Immunoblotting. Electrophoresis samples containing 100 mM dithiothreitol were incubated at 37°C for 15 min before gel electrophoresis. The procedure for immunoblotting was conducted as described previously (Pickering et al., 1995).

Molecular Modeling. A homology model of the closed form of the extracellular domain of human mGluR7 was generated using the X-ray crystal structure of the extracellular domain of rat mGluR1 as a template (Kunishima et al., 2000) (Protein Data Bank coordinates, 1EWK.pdb). The sequence alignment between the rat mGluR1 and human mGluR7 sequences was adopted from the multiple alignment of the eight mGluRs (Fig. 2). The alignment was checked to avoid gap insertions in the conserved secondary structural motifs. MODELER 6 (Sali and Blundell, 1993) was used to generate the homology model, and SYBYL 6.9 (Tripos, St. Louis, MO) was used to view, analyze, and manipulate the structure. The short disordered loop absent in the crystal structure of mGluR1 was excluded from the model. The MODELER and VERIFY 3D servers (Luthy et al., 1992) were used to assess the integrity of the model. The best initial model was subjected to further refinement using energy minimization with AMBER 7.0 (Case et al., 2001). The force-field parameters for the ligands were developed with the aid of the antechamber module in AMBER. The coordinates for the zwitterionic forms of glutamate and L-AP4 were generated in an extended conformation using the Xleap module in AMBER 7.0. The ionization state of the phosphate group of L-AP4 was PO_3^{-2}.

The mGluR7 homology model was first energy-minimized with glutamate docked in the same orientation as in the mGluR1 crystal structure. The complex was solvated in a TIP3P water box (Jorgensen et al., 1983) so that the box boundaries were at least 10 Å away from any protein atom. A water molecule in the crystal structure of mGluR1 between the bound glutamate and arginine 78 was retained in the mGluR7 model because this amino acid is conserved in all mGluRs. Additional water molecules were placed in the binding pocket by solvation using AMBER. Although the placement of the water molecules in the binding pocket causes a negative and thus unfavorable change in entropy, this procedure optimizes the interactions between the ligand and the receptor. Counter ions (Cl^-) were added to neutralize the system. The coordinates for the solvated complex were then energy-minimized in AMBER 7.0 using the Cornell force field. A dielectric multiplicative constant of 1.0 was used to calculate the electrostatic interactions, and a cutoff of 12 Å was used for nonbonding interactions. The final energy minimization was carried out by restraining the protein backbone and then reducing the constraints gradually to zero. Thereafter, the model was minimized for 5000 steps without constraints. The bound glutamate was replaced by L-AP4, and the mGluR7-L-AP4 complex was energy-minimized as described above.

Results

Pharmacological Profiles of mGluR4, mGluR6, and mGluR7. In heterologous expression systems, the group III mGluRs are coupled to the inhibition of adenylyl cyclase. To switch the signal transduction system to the stimulation of phosphoinositide turnover and release of intracellular calcium, the receptor cDNAs were transiently cotransfected with the cDNA coding for the promiscuous Gα15 G-protein subunit to artificially couple the receptor to the phospholipase C pathway (Gomeza et al., 1996). L-AP4–induced responses were monitored by measuring the release of intracellular calcium in HEK cells loaded with the calcium-sensitive dye Fluo-4. The EC_{50} values for L-AP4 for mGluR4 and mGluR6 were 0.29 ± 0.03 and 1.97 ± 0.59 μM, respectively (Fig. 3). In contrast, no responses were observed in cells coexpressing either rat or human mGluR7 and Gα15 (or the chimeric G-protein Gqi9) with concentrations of L-AP4 up to 500 μM. However, responses were consistently obtained in HEK cells cotransfected with Gα15 and a construct in which the first the first 44 amino acids of the human mGluR7 receptor were replaced with the first 27 amino acids of the human CaSR; the EC_{50} value for L-AP4 was 429 ± 134 μM.

Analysis of Chimeras of mGluR4 and mGluR6. We reported previously that in HEK cells expressing mGluR4, high levels of [^{3}H]L-AP4 binding were observed, whereas [^{3}H]L-AP4 binding was undetectable in HEK cells expressing mGluR6 or mGluR7 (Naples and Hampson, 2001). This experiment was repeated, and the results were confirmed in the present study. To identify the region within the mGluR6 receptor responsible for the inhibition of [^{3}H]L-AP4 binding, chimeric receptors containing portions of the extracellular domain of mGluR4 were ligated to the complementary downstream segments of mGluR6 (Fig. 3). Membranes prepared from cells expressing the mGluR4/6 chimeras and the mGluR6 wild-type receptor were probed on immunoblots with a C-terminal anti-mGluR6 antibody; the mGluR6 receptor was highly expressed, whereas the chimeras were expressed at lower levels (Fig. 4).

The mGluR4/6A chimera encompassed the complete extracellular domain of mGluR4 (amino acids 1–586) spliced to the transmembrane and C-terminal regions of mGluR6 (amino acids 579–871). Autocompetition radioligand binding experiments with labeled and unlabeled L-AP4 showed that the mGluR4/6A chimera had an affinity for L-AP4 that was similar to that of wild-type mGluR4 (4/6A IC_{50} = 0.43 ± 0.04 μM; mGluR4 IC_{50} = 0.35 ± 0.10 μM) (Fig. 3). However, in the functional assay, the 4/6A chimera was not activated by L-AP4 at concentrations of up to 500 μM. The lack of activity with the m4/6A chimera could have been caused by the two amino acid change at the junction of the extracellular domain and the transmembrane domain region in the construction of this chimera. However, it should be noted that other nonfunctional chimeras have also been observed in other family C receptors [e.g., mGluR2/mGluR1 (Takahashi et al., 1993), mGluR1/DmGluRA (Parmentier et al., 1998), $GABA_BR1$/mGluR1 (Malitschek et al., 1999), and mGluR1/4 (Maj et al., 2003)].

The mGluR4/6B chimera contained the first 110 amino acids of mGluR4 spliced to amino acids 95 to 871 of mGluR6, the mGluR4/6C chimera contains the first 78 amino acids of mGluR4 spliced to amino acids 63 to 871 of mGluR6, and the mGluR4/6D chimera contains the first 50 amino acids of mGluR4 spliced to amino acids 35 to 871 of mGluR6. All of these chimeras displayed affinities for L-AP4 similar to the wild-type mGluR4 receptor in the autocompetition binding assay and in the functional assay (Fig. 3). These findings indicate that the region of the mGluR6 receptor responsible for the lack of [^{3}H]L-AP4 binding is located within the first 35 amino acids of the mGluR6 receptor.

The Affinity of L-AP4 for Activation of mGluR6 Is Influenced by Amino Acids within the Ligand Binding Pocket. To explore the ligand binding pocket of mGluR6, amino acids that establish bonds with agonists in the binding pocket were mutated to alanine residues. We previously generated a structural model of mGluR4 with L-SOP docked into the binding pocket (Rosemond et al., 2002) derived from the crystal structure of mGluR1 (Kunishima et al., 2000; Tsuchiya et al., 2002). Two amino acids within the binding pockets differ between mGluR4 and mGluR6; lysine 74 and glycine

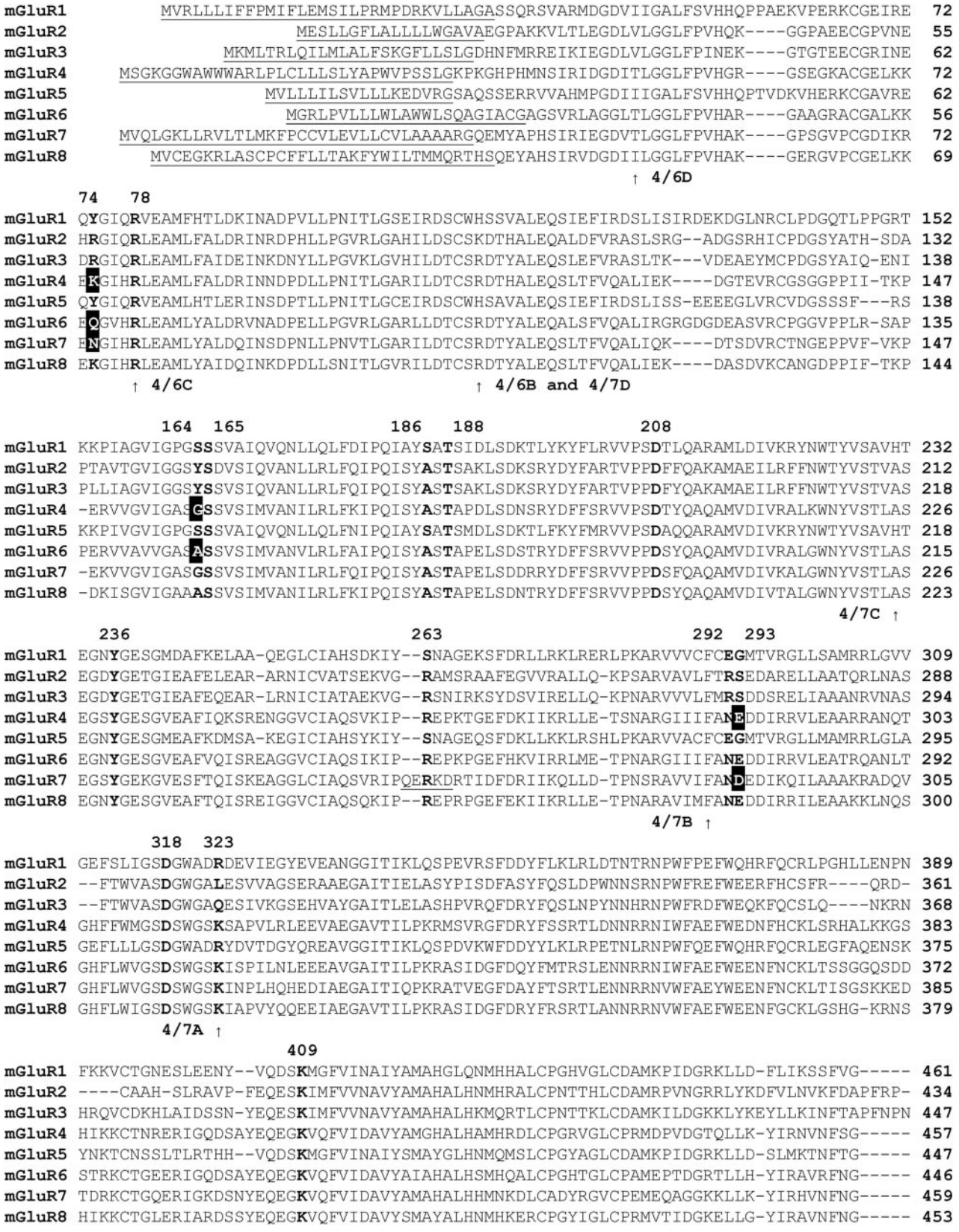

Fig. 2. Multiple sequence alignment of a portion of the extracellular domains of mGluRs. The alignment was generated using ClustalW version 1.8. Amino acids in boldface type are in the glutamate binding pocket; the numbers above the residues indicate amino acids in mGluR1. Amino acids highlighted with a black background represent residues in the ligand binding pocket that differ between mGluR4 and mGluR6 (Q58 and A159 of mGluR6) and mGluR4 and mGluR7 (N74 and D289 of mGluR7). The proposed loop region mGluR7 (encompassing glutamine 258 to aspartate 262) that was mutated is underlined. Ligation sites for the receptor chimeras are indicated by the arrows, and the predicted signal peptides are underlined. The sequences shown are the rat sequences except for mGluR7, which is the human sequence. Within the region shown, the human mGluR7 sequence differs from the rat sequence at two amino acids (G5R and V27A, rat to human).

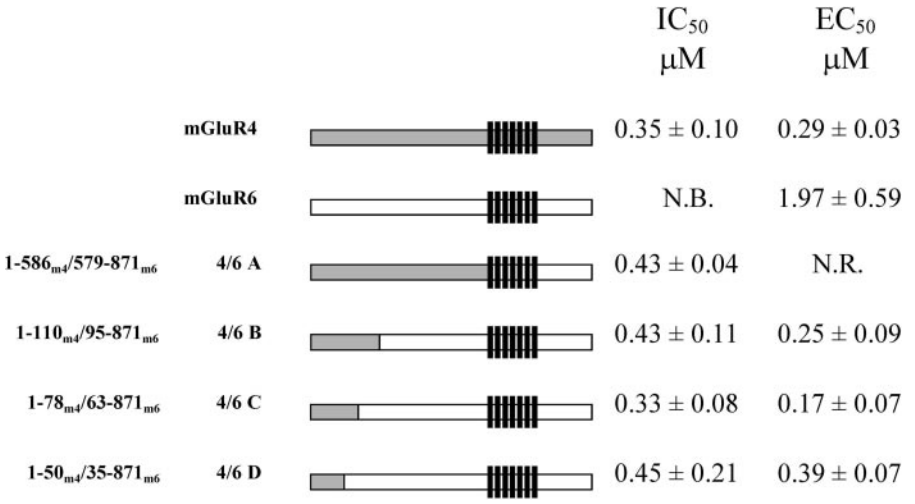

Fig. 3. Radioligand binding and functional analysis of mGluR4/mGluR6 receptor chimeras. IC_{50} values were calculated from [^{3}H]L-AP4 radioligand binding experiments, whereas EC_{50} values were generated from the fluorescence-based functional assay. All values are the means ± S.E.M. of three to six experiments. N.B., no binding detected; N.R., no response with 500 μM L-AP4.

158 in mGluR4 correspond to glutamine 58 and alanine 159 in mGluR6 (Fig. 2). The mGluR6 Q58K/A159G double mutant displayed a 7-fold higher affinity for L-AP4 in the functional assay (EC_{50} = 0.27 ± 0.14 μM) compared with the wild-type mGluR6 receptor with an affinity that was similar to wild-type mGluR4. It is surprising, however, that the Q58K/A159G mutant showed no specific [^{3}H]L-AP4 binding despite the high level of protein expression observed on immunoblots (data not shown).

Analysis of mGluR7. To identify regions of the extracellular domain of mGluR7 receptor responsible for the low affinity of this receptor for agonists, four chimeras of mGluR4 and mGluR7 were studied (Fig. 5). The mGluR4/7A chimera included the first 315 amino acids of rat mGluR4 spliced to amino acids 317 to 915 of mGluR7. This chimera displayed a similar affinity for [^{3}H]L-AP4 in the binding assay and a relatively small 2.5-fold decrease in affinity for L-AP4 in the functional assay compared with wild-type mGluR4. The mGluR4/7B chimera contained the first 286 amino acids of mGluR4 spliced to amino acids 288 to 915 of mGluR7 and showed a 3-fold lower affinity for L-AP4 compared with mGluR4 (EC_{50} = 0.94 ± 0.23 μM). The mGluR4/7C chimera contained the first 221 amino acids of mGluR4 spliced to amino acids 222 to 915 of mGluR7; this construct showed a 10-fold decrease in affinity in the functional assay (EC_{50} = 3.02 ± 0.52 μM) compared with the wild-type mGluR4 receptor and a complete loss of detectable [^{3}H]L-AP4 binding. The mGluR4/7D chimera contained the first 110 amino acids of mGluR4 spliced to amino acids 109 to 915 of mGluR7. Despite robust expression on immunoblots (Fig. 4B), no specific [^{3}H]L-AP4 binding or activation by L-AP4 was observed in this construct with concentrations of up to 500 μM (Fig. 5).

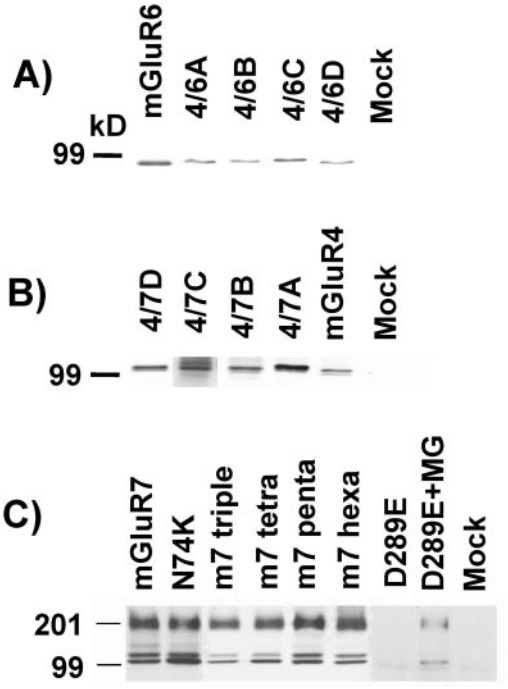

Fig. 4. Immunoblots of group III mGluR chimeras and point mutations. A, immunoblots of wild-type mGluR6 and the mGluR4/6 chimeras probed with an anti-mGluR6 antibody. B, immunoblots of the mGluR4/7 chimeras probed with the anti-mGluR7 antibody. C, immunoblots of mGluR7 mutations.

A homology model of mGluR7 was generated to facilitate further analysis of L-AP4 interactions at this receptor. The degree of amino acid sequence identity between mGluR7 and the template (mGluR1) within the region modeled was 41%. The model indicated that the ligand binding pocket of mGluR7 differs from mGluR4 by two residues: asparagine 74 in mGluR7 is a lysine in mGluR4, and aspartate 289 in mGluR7 is a glutamate in mGluR4 (Figs. 2 and 6). To our surprise, conservatively mutating aspartate 289 in mGluR7 to glutamate caused a complete loss of detectable protein on immunoblots; however, this mutant was detected when the cells were incubated with the proteosome inhibitor MG-132 before analysis on SDS-polyacrylamide gel electrophoresis (Fig. 4C). In contrast to D289E, converting asparagine 74 in mGluR7 to lysine increased the affinity for L-AP4 by 12-fold (EC_{50} = 35.6 ± 14 μM) (Table 1) compared with the unmutated mGluR7 receptor.

In addition to the two residues in the binding pocket, the homology model also indicated that a short segment encompassing amino acids glutamine 258 to aspartate 262 ($Q_{258}E_{259}R_{260}K_{261}D_{262}$) in mGluR7 differs between mGluR7 and the other group III receptors. This difference is readily apparent when the carbon backbone derived from the mGluR7 model is overlaid onto the structural model of mGluR4, where it can be seen that this stretch of residues forms a small loop in mGluR7 that is not present in the other

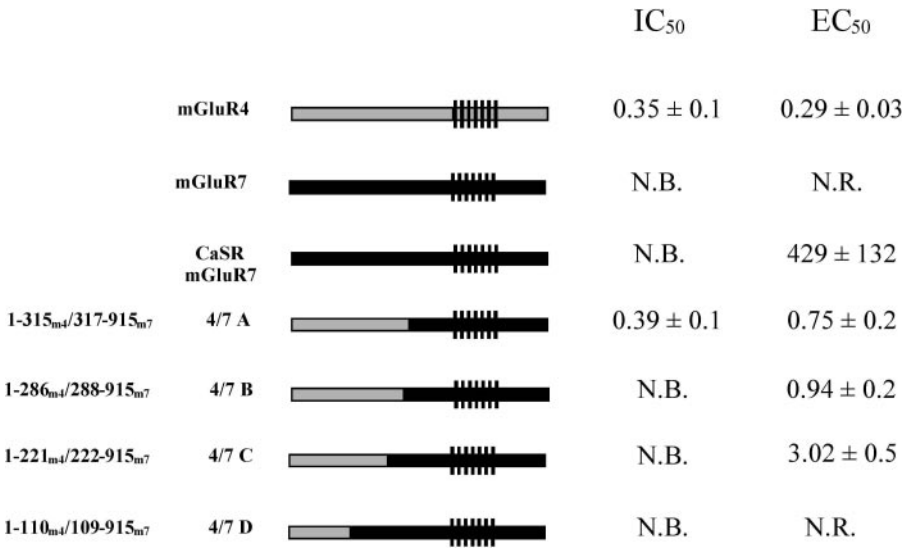

Fig. 5. Radioligand binding and functional analysis of mGluR4/mGluR7 receptor chimeras. [^{3}H]L-AP4 binding and L-AP4 activation studies of wild-type and mGluR4/7 receptor chimeras. All values are the means ± S.E.M. of three to five experiments. N.B., no binding detected; N.R., no response at 500 μM L-AP4.

group III receptors (Fig. 7). This five-amino acid segment in mGluR7 is represented by only three amino acids in the other group III receptors. We hypothesized that although this section of the polypeptide lies just outside of the binding pocket, it may influence ligand affinity. Therefore, the two extra residues in mGluR7 were deleted (glutamine 258 and glutamate 259, termed the QE deletion mutant), and then further mutants were produced that combined the QE deletion mutant with additional mutations in mGluR7 designed to mimic mGluR4. These included a triple mutant (QE deletion + K261E), a tetramutant (QE deletion + K261E and D262P), a pentamutant (QE deletion + K261E + D262P + N74K), and a hexamutant (QE deletion + K261E + D262P + N74K + D289E).

The mutants were analyzed in the fluorescence-based functional assay, and the results are summarized in Table 1. All of the mutants in this series displayed affinities that were higher than the unmutated mGluR7 except for the QE deletion mutant, in which no responses were seen. The highest affinity mutant was the pentamutant (EC_{50} = 3.8 ± 0.8 μM), which included the deletion of two residues (Q258 and E259) and the replacement of two residues (K261E + D262P) in the loop region and replacement of one residue in the binding pocket (N74K). The hexamutant, which included the five amino acids in the pentamutant plus the second binding pocket mutation D289E, showed a lower affinity (EC_{50} = 9.3 ± 0.22 μM) compared with the pentamutant.

TABLE 1
EC_{50} values for the mGluR7 mutants
All values, in micromolars, are the means ± S.E.M. of three to five determinations.

mGluR7	429 ± 132
N74K	35.6 ± 14
QE del + K261E (Triple mutant)	243.4 ± 104
QE del + K261E + D262P (tetramutant)	81.5 ± 47
QE del + N74K + K261E + D262P (pentamutant)	3.8 ± 0.8
QE del + N74K + K261E + D262P + D289E (hexamutant)	9.3 ± 2.2

QE del, deletion of glutamine 258 and glutamate 259 in mGluR7.

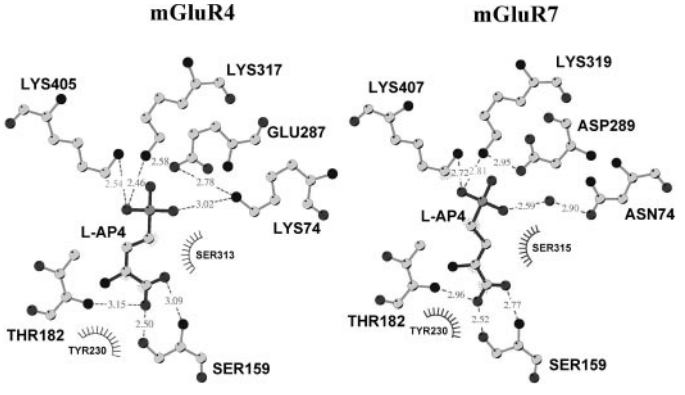

Fig. 6. Comparative schematic diagrams of the ligand binding pockets of mGluR4 and mGluR7. These schematic diagrams illustrate the differences in the interactions of L-AP4 at mGluR4 and mGluR7. Hydrogen-bonding distances are labeled in angstroms. For clarity, the interactions between the α-amino group of L-AP4 and the receptors are omitted. The diagram was produced using LIGPLOT (Wallace et al., 1995).

Fig. 7. Three-dimensional folds of the extracellular domains of mGluR4 and mGluR7. Ribbon structures of the backbones of the closed forms of mGluR4 (red) and mGluR7 (blue) are superimposed on each other, with glutamate docked into the ligand-binding pocket (depicted as a space-filled representation). The small loop region mutated in mGluR7 is colored in yellow.

Discussion

Glutamate- and GABA-mediated excitatory and inhibitory synaptic transmission are tightly regulated processes. In the central nervous system, group III mGluRs are present on both glutamatergic neurons and GABAergic interneurons (Shigemoto et al., 1996; Bradley et al., 1999; Corti et al., 2002), the latter of which are believed to be activated by glutamate "spillover" from nearby glutamatergic terminals (Mitchell and Silver, 2000; Semyanov and Kullmann, 2000). The precise amount of glutamate and GABA released is determined in part by the presence of the different subtypes of presynaptic mGluRs. Thus, the affinity of a presynaptic mGluR for glutamate is a critical factor in regulating synaptic neurotransmitter levels.

We proposed previously that the inhibitory properties of mGluR4 on neurotransmitter release are an important parameter in maintaining the appropriate level of neuronal firing during synaptic transmission (Pekhletski et al., 1996). High-affinity receptors such as mGluR4 and mGluR8 would be activated at low levels of synaptic activity, whereas high-frequency neuronal firing would be required to activate the low-affinity mGluR7 receptor (Sansig et al., 2001). Results from more recent studies also indicate that some L-AP4–sensitive receptors are tonically activated by resting levels of extracellular glutamate (Xi et al., 2003; Acuna-Goycolea et al., 2004).

The results from the present study provide an explanation for the molecular basis of the differential agonist affinities of the group III mGluRs. A side-by-side comparison of mGluR4, mGluR6, and mGluR7 expressed in HEK cells indicated that in the functional assay, wild-type mGluR4 and mGluR6 showed robust activity, whereas no receptor activation was observed with either rat or human mGluR7. The inability to detect responses to mGluR7 was probably not caused by a lack of cell surface expression because immunocytochemical analysis showed surface expression in fixed transfected HEK cells (data not shown). However, when the first 35 amino acids of mGluR7 were replaced with the first 44 amino acids of the CaSR, receptor activation was observed at concentrations of L-AP4 at and greater than 250 μM. Thus, the rank order of the EC_{50} values was mGluR4 $>$ mGluR6 $\gg$ mGluR7. However, as reported previously (Naples and Hampson, 2001), only mGluR4 (and mGluR8) displayed specific [^{3}H]L-AP4 binding.

The absence of [^{3}H]L-AP4 binding in mGluR7 can be explained by its extremely low affinity for agonists. The measured affinity for mGluR6 in the functional assay (EC_{50} = 1.9 μM) also suggests the possibility that the affinity of L-AP4 for mGluR6 was lower than the limit of detection in the binding assay. However the mGluR6 double mutant, which mimicked the binding pocket of mGluR4, increased the affinity of L-AP4 in the functional assay to that of mGluR4, yet this mutant still did not display [^{3}H]L-AP4 binding. It was surprising that high-affinity binding could be imparted to mGluR6 by replacing the first 35 amino acids with the first 50 amino acids of mGluR4. Although the homology models did not encompass most of this section of the receptor polypeptide because it is not part of the crystal structure of mGluR1 used as template in the model, it is believed that this region, which includes the predicted signal peptide sequence, lies well outside of the ligand binding pocket.

It is not clear how the amino terminus of the receptor could modulate high-affinity agonist binding. It has been reported that the extreme amino terminus of the GluR1 glutamate-gated α-amino-3-hydroxy-5-methyl-4-isoxazolepropionic acid receptor channel was required for proper trafficking to the plasma membrane (Xia et al., 2002). However, functional responses were obtained with mGluR6 in live HEK cells, and an immunocytochemical analysis showed that mGluR6 was expressed on the surface of transfected cells (data not shown); thus, aberrant receptor trafficking does not provide an explanation for the lack of detectable [^{3}H]L-AP4 binding in mGluR6.

Another possibility is that proper processing and cleavage of the signal peptide may be required for maintaining a high-affinity conformation of the receptor, or alternatively, the extreme amino terminus of the mature receptor, excluding the putative cleaved signal peptide sequence, may indirectly affect the precise 3-dimensional architecture of the binding pocket and therefore ligand affinity. We note that the importance of the first 30 to 50 residues in the group III mGluRs is also reflected in the observation that replacement of this region in mGluR7 with amino acids of the CaSR was required for generating functional responses to mGluR7 in HEK cells. Taken together, these findings indicate that the extreme amino termini contribute to the tertiary structure and pharmacological properties the group III mGluRs.

The molecular basis for the very low affinity of mGluR7 was first examined in a series of chimeras between mGluR4 and mGluR7. A pharmacological profile roughly similar to that of mGluR4 was seen in the mGluR4/7A chimera that contained the first 315 amino acids of mGluR4 ligated to the complementary downstream sequence of mGluR7. The mGluR4/7B and mGluR4/7C chimeras had progressively smaller segments of mGluR4 and displayed affinities in the functional assay that were 3- and 10-fold lower than mGluR4, respectively.

The mGluR4/7A chimera included the only two residues in the ligand binding pocket of mGluR4 that differ between the two receptors: asparagine 74 and aspartate 289 in mGluR7 align with lysine 74 and glutamate 287 in mGluR4. To determine the contribution of these two residues to the affinity of L-AP4, we generated and characterized the mGluR7 mutants N74K and D289E. The N74K mutant displayed a 12-fold increase in affinity over wild-type mGluR7, whereas the D289E mutant was undetectable on immunoblots unless a proteosome inhibitor was present. This latter observation indicates that the D289E mutant was rapidly degraded.

The largest mutagenesis-induced shift to higher affinity in mGluR7 was seen in the pentamutant, in which four residues comprising a small loop outside of the binding pocket and the binding pocket residue asparagine 74 were mutated to the equivalent amino acids in mGluR4. This loop region is situated on the top of lobe II just outside of the pocket containing the docked ligand and protrudes into the cavity formed by the two lobes of the Venus flytrap (Fig. 7). The data suggest that this loop or "bump" in the polypeptide chain contributes to the lower agonist affinity of mGluR7. The residues in this region may perturb the binding pocket residues that make direct contact with the bound ligand such that they establish less favorable contacts with the ligand compared with the high-affinity L-AP4 receptors. Alternatively, the protrusion of this loop into the cavity formed by the two lobes may hinder

full closure of the lobes in the Venus flytrap domain. This scenario is consistent with a previous proposal that ligand affinity depends in part on the propensity of the ligand to stabilize the closed conformation of the Venus flytrap (Parmentier et al., 2002).

Our results also clearly demonstrate that a primary contributor to agonist affinity in the group III mGluRs is the single position occupied by lysine 74 in mGluR4, glutamine 58 in mGluR6, and asparagine 74 in mGluR7 (Figs. 6 and 8). The amino acids occupying this position are also variable in the other members of the mGluR family (i.e., a tyrosine in group I receptors and an arginine in group II receptors) (Fig. 2). We suggest that the higher affinity of mGluR4 (and mGluR8) is mediated in part by an ion pair formed between lysine 74 in mGluR4 (and lysine 71 in mGluR8) and the phosphonate group of L-AP4 and L-SOP, and that the lower affinity of mGluR6 is caused by the replacement of the charged lysine with polar glutamine, which probably establishes a lower-energy hydrogen bond with the phosphonate group (Fig. 8). In mGluR7, we propose that a water molecule could link the oxygen atoms of the phosphonate group on L-AP4 and aspargine 74. In the homology model, the distance between these two oxygens is 4.3 Å, which is sufficient to accommodate a water molecule as shown in Fig. 8. Although the longer length of the charged side chain of lysine 74 in this position in mGluR4 precludes the presence of a water molecule, this residue probably establishes a direct interaction with the ligand that may contribute to the higher agonist affinity of this receptor. We predict that the various residues occupying this position in the mGluRs would be good candidates for structure-based drug-design efforts seeking to optimize ligand selectivity and affinity.

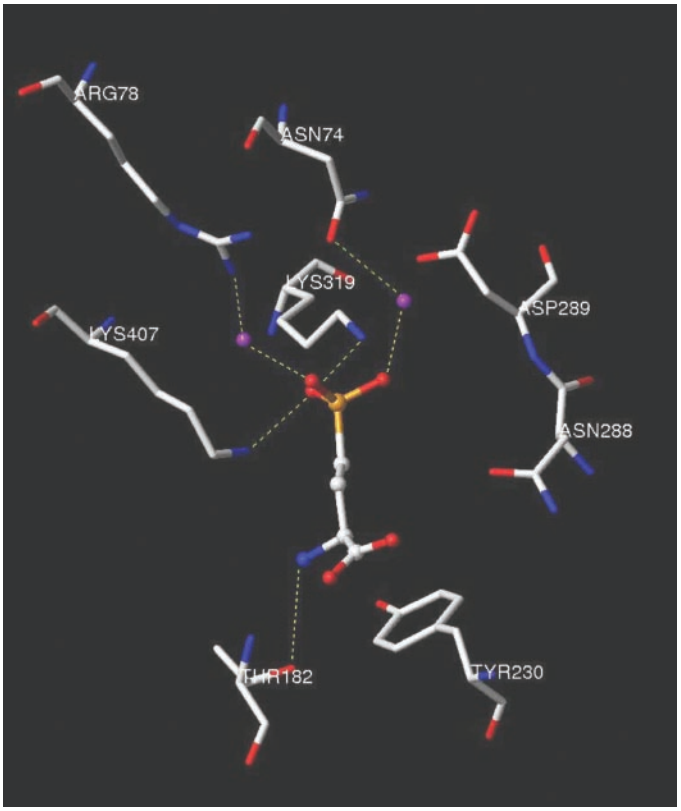

Fig. 8. Close up of the ligand-binding pocket of mGluR7. L-AP4 is docked into the binding pocket. Blue indicates nitrogen atoms; red, oxygen; orange, phosphorous; and purple spheres, water molecules. Selected hydrogen bonds are depicted as broken yellow lines. Water molecules link the side chains of arginine 78 and asparagine 74 to the phosphonate side chain of the bound L-AP4; the water linking arginine 78 with the ligand is consistent with its presence in this position in the mGluR1 crystal structure, whereas the water molecule linking asparagine 74 with L-AP4 is hypothetical and is proposed from the homology model and the mutagenesis data as detailed in the text.

Acknowledgments

We thank Drs. S. Nakanishi and M. Simon for the rat mGluR and Gα15 cDNAs. We are also grateful for the support of the supercomputing facility at the Molecular Design and Information Technology Centre in the Department of Pharmaceutical Sciences, University of Toronto.

References

Acuna-Goycolea C, Li Y, and van den Pol AN (2004) Group III metabotropic glutamate receptors maintain tonic inhibition of excitatory synaptic input to hypocretin/orexin neurons. *J Neurosci* **24:**3013–3022.

Ahmadian H, Nielsen B, Brauner-Osborne H, Johansen TN, Stensbol TB, Slok FA, Sekiyama N, Nakanishi S, Krogsgaard-Larsen P, and Madsen U (1997) (S)-Homo-AMPA, a specific agonist at the mGlu6 subtype of metabotropic glutamate receptors. *J Med Chem* **40:**3700–3705.

Bertrand H-O, Bessis A-S, Pin J-P, and Archer AC (2002) Common and selective molecular determinants involved in metabotropic glutamate receptor agonist activity. *J Med Chem* **45:**3171–3183.

Bessis A-S, Rondard P, Gaven F, Brabet I, Triballeau N, Prezeau L, Acher F, and Pin J-P (2002) Closure of the Venus flytrap module of mGlu8 receptor and the activation process: Insights from mutations converting antagonists into agonists. *Proc Natl Acad Sci USA* **99:**11097–11102.

Bradley SR, Standaert DG, Rhodes KJ, Rees HD, Testa CM, Levey AI, and Conn PJ (1999) Immunohistochemical localization of subtype 4a metabotropic glutamate receptor in the rat and mouse basal ganglia. *J Comp Neurol* **407:**33–46.

Bruno V, Ksiazek I, Battaglia G, Van der Putten H, Lukic S, Leonhardt T, Inderbitzin W, Gasparini F, Kuhn R, Hampson DR, et al. (2000) Selective activation of mGlu4 metabotropic glutamate receptors is protective against excitotoxic neuronal death. *J Neurosci* **20:**6413–6420.

Case DA, Pearlman DA, Caldwell JW, Cheatham TE III, Wang J, Ross WS, Simmerling C, Darden T, Merz KM, Stanton RV, et al. (2001) *AMBER,* version 7.0, University of California, San Francisco.

Corti C, Aldegheri L, Somogyi P, and Ferraguti F (2002) Distribution and synaptic localization of the metabotropic glutamate receptor 4 in the rodent CNS. *Neuroscience* **110:**403–420.

Corti C, Restituito S, Rimland JM, Brabet I, Corsi M, Pin J-P, and Ferraguti F (1998) Cloning and characterization of alternative mRNA forms for the rat metabotropic glutamate receptors mGluR7 and mGluR8. *Eur J Neurosci* **10:**3629–3641.

Cryan JF, Kelly PH, Neijt HC, Sansig G, Flor PJ, and van Der Putten H (2003) Antidepressant and anxiolytic-like effects in mice lacking the group III metabotropic glutamate receptor mGluR7. *Eur J Neurosci* **17:**2409–2417.

Gomeza J, Mary S, Brabet I, Parmentier M-L, Restituito S, Bockaert J, and Pin J-P (1996) Coupling of metabotropic glutamate receptors 2 and 4 to $G\alpha_{15}$, $G\alpha_{16}$ and chimeric $G\alpha_{q/I}$ proteins: characterization of new antagonists. *Mol Pharmacol* **50:**923–930.

Hampson DR, Huang X-P, Pekhletski R, Peltekova V, Hornby G, Thomsen C, and Thogersen H (1999) Probing the ligand-binding domain of the mGluR4 subtype of metabotropic glutamate receptor. *J Biol Chem* **274:**33488–33495.

Han G and Hampson DR (1999) Ligand binding to the amino-terminal domain of the mGluR4 subtype of metabotropic glutamate receptor. *J Biol Chem* **274:**10008–10013.

Jingami H, Nakanishi S, and Morikawa K (2003) Structure of the metabotropic glutamate receptor. *Curr Opin Neurobiol* **13:**271–278.

Jorgensen WL, Chandrasekhar J, Madura J, Impley RW, and Klein ML (1983) Comparison of simple potential functions for simulating liquid water. *J Chem Phys* **79:**926–935.

Kuang D, Yao Y, Wang M, Pattabiramann N, Kotra L, and Hampson DR (2003) Molecular similarities in the ligand binding pockets of an odorant receptor and the metabotropic glutamate receptors. *J Biol Chem* **278:**42551–42559.

Kunishima N, Shimada Y, Tsuji Y, Sato T, Yamamoto M, Kumasaka T, Nakanishi S, Jingami H, and Morikawa K (2000) Structural basis of glutamate recognition by a dimeric metabotropic glutamate receptor. *Nature (Lond)* **407:**971–977.

Lafon-Cazal M, Viennois G, Kuhn R, Malitschek B, Pin J-P, Shigemoto R, and Bockaert J (1999) mGluR7-like metabotropic glutamate receptors inhibit NMDA-mediated excitotoxicity in cultured mouse cerebellar granule neurons. *Neuropharmacology* **38:**1631–1640.

Luthy R, Bowie JU, and Eisenberg D (1992) Assessment of protein models with three-dimensional profiles. mGluR7-like metabotropic glutamate receptors inhibit NMDA-mediated excitotoxicity in cultured mouse cerebellar granule neurons. *Nature (Lond)* **356:**83–85.

Macchiarulo A, Costantino G, Shaglia R, Stefania A, Meniconi M, and Pellicciari R (2003) The role of electrostatic interaction in the molecular recognition of selective agonists to metabotropic glutamate receptors. *Proteins* **50:**609–619.

Macek TA, Winder DG, Gereau RW, Ladd CO, and Conn PJ (1996) Differential involvement of group II and group III mGluRs as autoreceptors at lateral and medial perforant path synapses. *J Neurophysiol* **76:**3798–3806.

Maj M, Bruno V, Dragic Z, Yamamoto R, Battaglia G, Inderbitzin W, Stoehr N, Stein T, Gasparini F, Vranesic I, et al. (2003) (−)-PHCCC, a positive allosteric modulator of mGluR4: characterization, mechanism of action and neuroprotection. *Neuropharmacology* **45:**895–906.
Malitschek B, Schweizer C, Keir M, Heid J, Froestl W, Mosbacher J, Kuhn R, Henley J, Joly C, Pin J-P, et al. (1999) The N-terminal domain of gamma-aminobutyric $acid_B$ receptors is sufficient to specify agonist and antagonist binding. *Mol Pharmacol* **56:**448–454.
Marino MJ, Williams DL, O'Brien JA, Valenti O, McDonald TP, Clements MK, Wang R, DiLella AG, Hess JF, Kinney GG, et al. (2003) Allosteric modulation of group III metabotropic glutamate receptor 4: A potential approach to Parkinson's disease treatment. *Proc Natl Acad Sci USA* **100:**13668–13673.
Mitchell SJ and Silver RA (2000) Glutamate spillover suppresses inhibition by activating presynaptic mGluRs. *Nature (Lond)* **404:**498–501.
Nakajima Y, Iwakabe H, Akazawa C, Nawa H, Shigemoto R, Mizumo N, and Nakanishi S (1993) Molecular characterization of a novel retinal metabotropic glutamate receptor mGluR6 with high selectivity of L-2-amino-4-phosphonobutyrate. *J Biol Chem* **268:**11868–11873.
Naples MA and Hampson DR (2001) Pharmacological profiles of the metabotropic glutamate receptor ligands [^{3}H]L-AP4 and [^{3}H]CPPG. *Neuropharmacology* **40:** 170–177.
Nomura A, Shigemoto R, Nakamura Y, Okamoto N, Mizuno N, and Nakanishi S (1994) Developmentally regulated postsynaptic localization of a metabotropic glutamate receptor in rat rod bipolar cells. *Cell* **77:**361–369.
Okamoto N, Hori S, Akazawa C, Hayashi Y, Shigemoto R, Mizuno N, and Nakanishi S (1994) Molecular characterization of a new metabotropic glutamate receptor mGluR7 coupled to inhibitory cyclic AMP signal transduction. *J Biol Chem* **269:** 1231–1236.
Parmentier ML, Joly C, Restituito S, Backaert J, Grau Y, and Pin JP (1998) The G-protein-coupling profile of metabotropic glutamate receptors, as determined with exogenous G proteins, is independent of their ligand recognition domain. *Mol Pharmacol* **53:**778–786.
Parmentier M-L, Prezeau L, Bockaert J, and Pin J-P (2002) A model for the functioning of family 3 GPCRs. *Trends Pharmacol Sci* **23:**268–274.
Pekhletski R, Gerlai R, Overstreet L, Huang X-P, Agoypan N, Slater NT, Abramow-Newerly W, Roder JC, and Hampson DR (1996) Impaired cerebellar synaptic plasticity and motor performance in mice lacking the mGluR4 subtype of metabotropic glutamate receptor. *J Neurosci* **16:**6364–6373.
Peltekova V, Han G, Soleymanlou N, and Hampson DR (2000) Constraints on proper folding of the amino terminal domains of group III metabotropic glutamate receptors. *Mol Brain Res* **76:**180–190.
Pickering DS, Taverna FA, Slater MW, and Hampson DR (1995) Palmitoylation of the GluR6 kainate receptor. *Proc Natl Acad Sci USA* **92:**12090–12094.
Rosemond E, Peltekova V, Naples M, Thogersen H, and Hampson DR (2002) Molecular determinants of high affinity binding to group III metabotropic glutamate receptors. *J Biol Chem* **277:**7333–7340.
Sali A and Blundell TL (1993) Comparative protein modelling by satisfaction of spatial restraints. *J Mol Biol* **234:**779–815.
Sansig G, Bushell T, Clarke VRJ, Rozov A, Burnashev N, Portet C, Gasparini F, Schmutz M, Klebs K, Shigemoto R, et al. (2001) Increased seizure susceptibility in mice lacking metabotropic glutamate receptor 7. *J Neurosci* **21:**8734–8745.
Saugstad JA, Kinzie JM, Mulvihill ER, Sergerson TP, and Westbrook GL (1994) Cloning and expression of a new member of the L-2-amino-4-phosponobutyric acid-sensitive class of metabotropic glutamate receptors. *Mol Pharmacol* **45:**367–372.
Schoepp DD, Jane DE, and Monn JA (1999) Pharmacological agents acting at subtypes of metabotropic glutamate receptors. *Neuropharmacology* **38:**1431–1476.
Semyanov A and Kullmann DM (2000) Modulation of GABAergic signaling among interneurons by metabotropic glutamate receptors. *Neuron* **25:** 663–672.
Shigemoto R, Kulik A, Roberts JDB, Ohishi H, Nusser Z, Kaneko T, and Somogyi P (1996) Target-cell-specific concentration of a metabotropic glutamate receptor in the presynaptic active zone. *Nature (Lond)* **381:**523–525.
Snead OC III, Banerjee PK, Burnham M, and Hampson D (2000) Modulation of absence seizures by the $GABA_A$ receptor: A critical role for metabotropic glutamate receptor 4 (mGluR4). *J Neurosci* **20:**6218–6224.
Takahashi K, Tsuchida K, Tanabe Y, Masu M, and Nakanishi S (1993) Role of the large extracellular domain of metabotropic glutamate receptors in agonist selectivity determination. *J Biol Chem* **268:**19341–19345.
Tsuchiya D, Kunishima N, Kamiya N, Jingami H, and Morikawa K (2002) Structural views of the ligand-binding cores of a metabotropic glutamate receptor complexed with an antagonist and both glutamate and Gd^+. *Proc Nat Acad Sci USA* **99:**2660–2665.
Wallace AC, Laskowski RA, and Thornton JM (1995) LIGPLOT: A program to generate schematic diagrams of protein-ligand interactions. *Protein Eng* **8:**127–134.
Xi Z-X, Shen H, Baker DA, and Kalivas PW (2003) Inhibition of non-vesicular glutamate release by group III metabotropic glutamate receptors in the nucleus accumbens. *J Neurochem* **87:**1204–1212.
Xia H, von Zastrow M, and Malenka RC (2002) A novel anterograde trafficking signal present in the N-terminal extracellular domain of ionotropic glutamate receptors. *J Biol Chem* **277:**47765–47769.
Yao Y, Pattabiraman N, Michne WF, Huang X-P, and Hampson DR (2003) Molecular modeling and mutagenesis of the ligand binding pocket of the mGluR3 subtype of metabotropic glutamate receptor. *J Neurochem* **86:**947–957.

Address correspondence to: Dr. David R. Hampson, University of Toronto, 19 Russell Street, Toronto, Ontario, Canada M5S 2S2. E-mail: d.hampson@utoronto.ca